frontiers | Frontiers in Energy Research

TYPE Original Research
PUBLISHED 11 July 2024
DOI 10.3389/fenrg.2024.1429256

OPEN ACCESS

EDITED BY
Yonghui Liu,
Hong Kong Polytechnic University, Hong Kong SAR, China

REVIEWED BY
Jun Huang,
Hebei University of Technology, China
Shun Sang,
Nantong University, China
Huimin Wang,
Zhejiang Sci-Tech University, China

*CORRESPONDENCE
Xiaoke Zhang,
zxk5511@126.com

RECEIVED 07 May 2024
ACCEPTED 14 June 2024
PUBLISHED 11 July 2024

CITATION
Zhang X, Wang J, Gao Z, Zhang S and Teng W (2024), Advanced strategy of grid-forming wind storage systems for cooperative DC power support.
Front. Energy Res. 12:1429256.
doi: 10.3389/fenrg.2024.1429256

Advanced strategy of grid-forming wind storage systems for cooperative DC power support

Xiaoke Zhang[1]*, Jiaqi Wang[2], Zan Gao[2], Shaofeng Zhang[1] and Weijun Teng[1]

[1]State Grid Henan Electric Power Research Institute, Zhengzhou, China, [2]School of Electrical Engineering, Xi'an Jiaotong University, Xi'an, China

Grid-forming (GFM) wind storage systems (WSSs) possess the capability of actively building frequency and phase, enabling faster frequency response. The frequency regulation power of GFM WSSs is provided by both the rotor of wind turbine and the battery storage (BS) in parallel with DC capacitor. However, with existing control strategies, the energy storage immediately responds to both small and large grid disturbances. The frequent responses significantly decrease the lifespan of energy storage. To address this issue, a cooperative strategy between rotor and energy storage is necessary. This paper proposes an advanced strategy of GFM WSSs for cooperative DC power support. The cooperative principle is that for small disturbances, the BS is disabled and total frequency regulation power is provided by the rotor, while for large disturbances, the BS is enabled to cooperatively provide power support with the rotor. The proposed cooperative strategy can decrease the charging and discharging times of BS with a small range of rotor speed fluctuation, and then the service life of BS can be significantly extended. Simulation results validate the effectiveness and superiority of the proposed strategy.

KEYWORDS

wind storage system, cooperative power support, grid forming control, battery storage, frequency regulation

1 Introduction

With the development of wind power generation, its penetration in grids is increasing (Liu et al., 2021; Bao et al., 2022; Huang et al., 2023). Currently, the predominant control method for most wind turbines is grid-following (GFL) control, which relies on a phase-locked loop (PLL) to synchronize with the frequency/phase of the AC grid. However, this approach faces challenges in maintaining stable operation under weak grid conditions and lacks grid support capability Xiong et al. (2020). Consequently, wind power systems utilizing grid-forming (GFM) control have obtained wide attention due to their capability of rapid frequency regulation (FR), facilitated to autonomously forming frequency/phase (Jiao and Nian, 2020; Zhao et al., 2021).

The FR of GFM wind power systems takes a frequency regulation (FR) cost of the frequency response resources (Xiong et al., 2019). Releasing the rotational kinetic energy of the rotor can enhance grid frequency stability (Lin and Liu, 2020). However, utilizing rotor power for FR purposes requires sacrificing the maximum power point tracking

(MPPT) of the wind power system and tapping into the limited amount of stored energy, thus somewhat diminishing the FR effect (Xiong et al., 2015). Battery storage (BS) offers notable advantages such as rapid response times and precise tracking of active power commands. Through optimized control system designs, wind farms can attain swift inertia response capabilities and continuous active power support, underscoring the necessity of equipping wind farms with a certain percentage of BS (Astero and Evens, 2020).

For wind storage systems (WSSs), scholars both domestically and internationally have proposed various control methods. In Shadoul et al. (2022), flywheel energy storage is integrated on the DC side of WSSs. Here, the BS assumes control over the DC bus voltage during grid-connected operation, facilitating virtual synchronous control of the grid-side converter. This approach ultimately enhances system inertia responsiveness, smoothens the active output of WSSs, and ensures the stability of the DC bus voltage. Yang et al. (2023) addresses the practical constraints of wind farms and BS systems, using model prediction to design WSSs for small-scale grid-oriented FR control. However, this strategy necessitates the determination of the grid inertia time constant, a parameter often challenging to ascertain in large grids. Mohamed et al. (2022) integrates considerations of DC voltage maintenance on the energy storage side and virtual synchronization control of the grid-side converter (GSC). Furthermore, it accounts for the load state of the BS and coordinates main unit control, converter control, and BS side control to maintain energy balance. This is achieved through rotational speed control of the machine-side converter (MSC) and adjustment of blade pitch angles to ensure energy equilibrium. Zeng et al. (2021) establishes a connection between the BS and the wind farm exit bus. It devises a strategy based on fuzzy control for the BS to emulate the FR inertia of the wind farm. However, this strategy overlooks the utilization of the frequency support capability inherent in WSSs. Sang et al. (2021) proposes a voltage source-type configuration network control method that utilizes DC-side energy. It integrates the concepts of virtual synchronous control and DC capacitor inertial synchronous control within the grid-side converter for WSSs equipped with additional supercapacitors on the DC-side. Additionally, it introduces a virtual capacitor control strategy in the supercapacitor storage-side converter. Sun et al. (2022) uses fuzzy control to devise a strategy for superconducting BS to aid wind turbines in MPPT operation, aiming to conserve BS capacity allocation. However, this strategy overlooks the potential coordination between BS and rotor kinetic energy to provide frequency support. Ahsan and Mufti (2020) investigates the coordination strategy of BS and wind turbines to deliver FR response. It explores scenarios based on whether the frequency rate of change meets FR power demand. This involves designing load shedding operations for WSSs to participate in FR control using fuzzy control. Meng et al. (2023) proposes a virtual synchronous generator cooperative control scheme for wind farms and their GFM BS devices on the AC side. This scheme enables the WSSs to function as a voltage source, providing both system damping and inertia. Yao et al. (2024) developed a wind farm FR model and an adaptive primary FR control strategy for a BS system, utilizing the frequency change rate as the output conversion characteristic. In summary, existing control methods for GFM WSSs often result in frequent actions of the energy storage, with insufficient consideration for the service life of the battery. Notably, the general design life of batteries is typically 4–5 years, a duration often insufficient for high FR demand scenarios (Dhiman and Deb, 2020).

To address the aforementioned challenges, this paper investigates the cooperative principle of DC power support in GFM WSSs and introduces a cooperative control strategy. The fundamental principle of the proposed control is as follows: for small disturbances, the BS is disabled and total frequency regulation power is provided by the rotor, while for large disturbances, the BS is enabled to cooperatively provide power support with the rotor. This control approach aims to minimize the time of BS charging and discharging, consequently enhancing the service life of BS, while ensuring minimal fluctuations in rotor speed.

The remaining sections of this manuscript are as follows. Section 2 describes the control methods for GFM WSSs. Section 3 analyzes the cooperative principle of DC-side power support in GFM WSSs and introduces a cooperative control strategy tailored for these systems. Finally, Section 4 validates the effectiveness and superiority of the proposed control method.

2 Control strategy of GFM WSS

As shown in Figure 1, the typical PMSG based GFM WSSs consists of wind generation modules and BS modules. Wind generation module mainly consists of wind turbine (WT), PMSG, MSC, dc-capacitor, and GSC. The BS module mainly consists of battery, battery storage converter (BSC).

2.1 GFM control strategy for WTs

The power balance relationship on the DC side of the WSSs is given by

$$P_{\mathrm{wt}} + P_{\mathrm{BS}} = P_{\mathrm{dcout}} = P_{\mathrm{w}} \tag{1}$$

where P_{BS} is the BS output power; P_{dcout} is the power released by the DC capacitor; P_{w} is the WSSs output power and P_{wt} is the wind power captured by WT, which is shown in Eq. 2,

$$P_{\mathrm{wt}} = \frac{1}{2}\rho\pi R_{\mathrm{w}}^2 C_{\mathrm{p}}(\lambda,\beta)\, v_{\mathrm{m}}^3 \tag{2}$$

where ρ is the air density; R_{w} is the blade radius of the wind turbine; C_{p} is the wind energy utilization coefficient; λ is the blade tip speed ratio; β is the pitch angle; and v_{w} is the inlet wind speed.

The MSC uses DC-link voltage control to stabilize the DC voltage, as depicted in Figure 2. In dc-link voltage strategy, the d-axis current command value i_{rdref} is set to 0, while the q-axis current command value i_{rqref} is determined by the DC capacitor voltage loop.

The GSC uses droop control to construct the voltage and frequency, which realizes the grid-configuration operation, as depicted in Figure 3. It should be noted that for GFM WSSs, the GFM control is implemented by the GSC. Consequently, WSSs output power is no longer determined by P_{wt} captured by WT, but depends on the grid load.

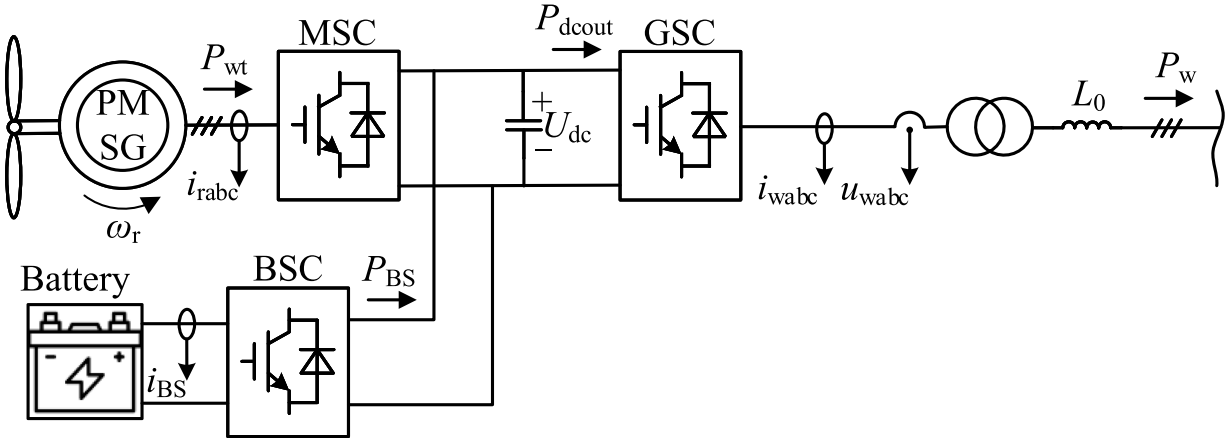

FIGURE 1
Circuit topology of GFM WSS.

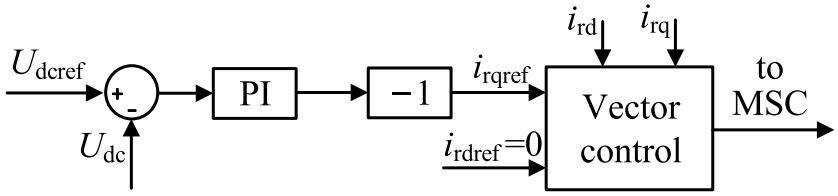

FIGURE 2
MSC control structure.

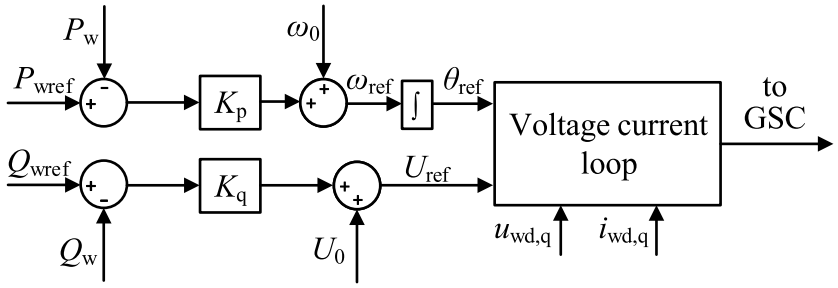

FIGURE 3
GSC control strategy.

Droop control simulates the active-frequency and reactive-voltage droop characteristics of a synchronous generator, and the control equations for its frequency and voltage are shown in Eq. 3,

$$\begin{cases} \omega_{ref} = \omega_0 + K_p(P_{wref} - P_w) \\ U_{ref} = U_0 + K_q(Q_{wref} - Q_w) \end{cases} \quad (3)$$

where ω_{ref} is the grid angular velocity reference value; ω is the grid angular velocity; ω_0 is the grid rated angular velocity; K_p is the active droop coefficient; P_{wref} is the WSSs rated output power; U_{wref} is the grid voltage reference value; U_0 is the rated grid voltage; K_q is the reactive droop coefficient; Q_w is the WSSs reactive power; Q_{wref} is the WSSs rated reactive power.

2.2 BS control strategy

GFM WSSs BS distribution methods include AC-side BS and DC-side BS. For the former, it can be considered as utilizing the BS system of GFM control to assist the operation of the wind generation systems, while the wind generation systems still adopt GFL control. The significant advantage of the DC-side BS in GFM WSSs is that the DC voltage can be stabilized with the help of an additional BS on the DC side, which effectively aids in realizing the GFM control of the turbine. Compared to the AC-side BS, the DC-side BS of WSSs can save one inverter, thus reducing the cost. Additionally, the DC-side BS is more integrated in structure and control, which

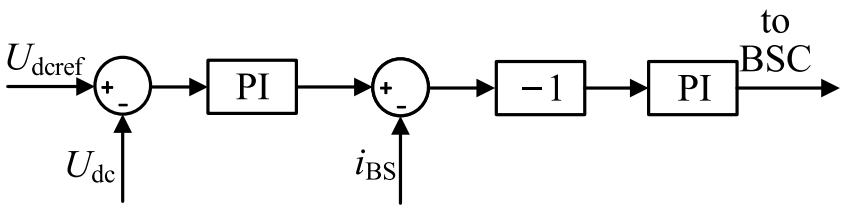

FIGURE 4
BSC control structure.

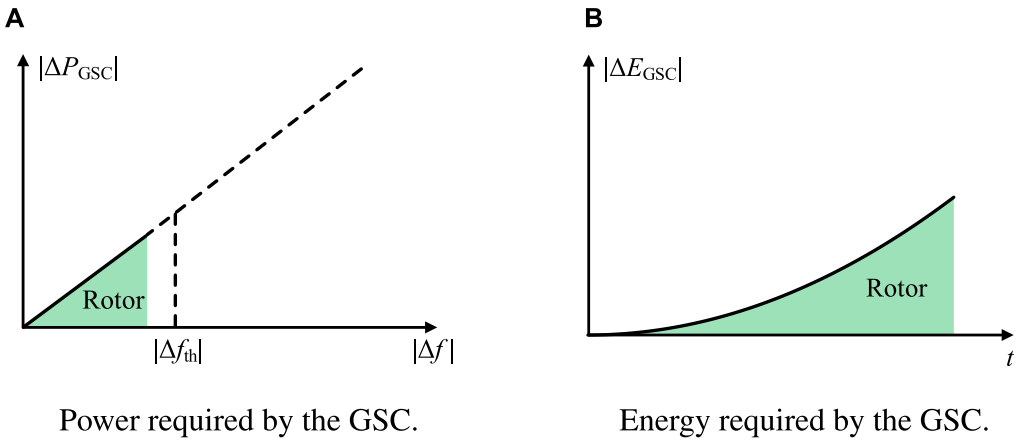

FIGURE 5
Small disturbance power support. **(A)** Power required by the GSC. **(B)** Energy required by GSC.

has the potential to enhance the transient and steady-state control capabilities of the unit and optimize its operational flexibility while meeting active support energy demand (Liu et al., 2020). Therefore, in this paper, the DC-side distribution BS is adopted to provide FR support power for the system.

The BSC control structure is shown in Figure 4. The current command value for the BS is derived from the DC capacitor voltage loop. Subsequently, the PWM control signal for the BSC is generated from the current loop.

2.3 Challenge of GFM WSSs

From Eq. 1, for wind generation systems without BS, in the event of a small disturbance, the system can respond by utilizing the wind turbine rotor to release or absorb energy, thereby adjusting rotational speed. However, during large disturbances, the spare power available from the rotor may not suffice to counteract the disturbance. Consequently, the energy supplied by the rotor to the DC capacitor may fail to match the energy it releases, resulting in instability of the capacitor voltage.

In conventional wind storage systems, the BS responds to disturbances of any magnitude, ensuring stabilization of the DC voltage and maintenance of rotor speed within normal ranges. However, frequent activation of the BS can lead to unnecessary wear and tear on the battery. Presently, the cycle life of Li-ion batteries ranges from 3,000 to 5,000 cycles. Excessive activation of the BS for each disturbance significantly shortens the battery's service life (Liu et al., 2020). Therefore, imprudent utilization of the BS can have adverse effects on the economic operation of the wind storage system.

In summary, to fulfill the system's power support requirements while minimizing the usage times of BS, there is a pressing need for a cooperative control strategy. This strategy aims to facilitate effective collaboration between the wind turbine rotor and the BS, enabling them to respond appropriately to varying degrees of disturbances encountered by the wind storage system within the power system.

3 Cooperative DC power support strategy of GFM WSS

3.1 Cooperative principle

From the analysis presented above, it becomes apparent that BS in WSSs should only be activated in response to large disturbances, while small disturbances do not necessitate their activation. It is not desirable for BS to respond to every disturbance encountered. Building upon this insight, this paper proposes a cooperative control strategy for DC-side power support in wind storage systems. This strategy utilizes frequency as a threshold to discern the size of the disturbance, determining when BS activation is warranted.

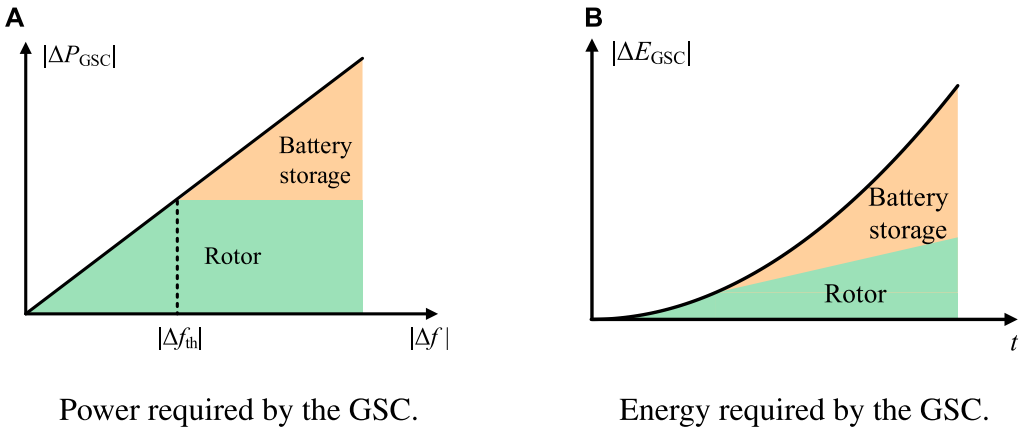

FIGURE 6
Large disturbance power support. **(A)** Power required by the GSC. **(B)** Energy required by GSC.

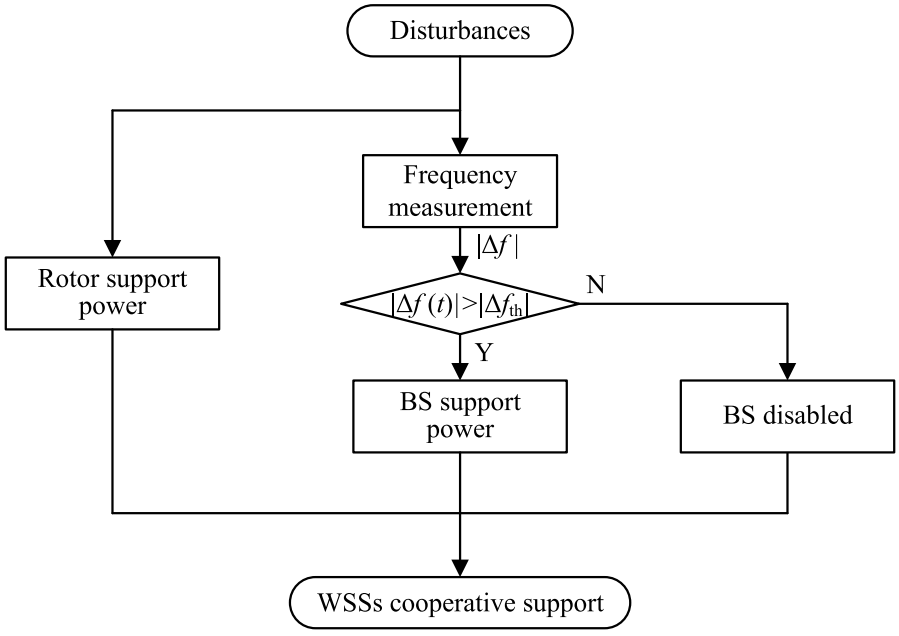

FIGURE 7
Cooperative principle of the cooperative control for GFM WSS.

When a disturbance results in a frequency deviation of the WSSs that is below the frequency threshold $|\Delta f_{th}|$, it is categorized as a small disturbance. In such cases, the BS does not respond, and the DC voltage is maintained stable solely by the rotor. Figure 5 illustrates the power and energy needed to support the GSC during small disturbances. As depicted in Figure 5A, the frequency deviation caused by small disturbances remains below the frequency threshold $|\Delta f_{th}|$, indicating that all the GSC power $|\Delta P_{GSC}|$ is sustained by the rotor. Figure 5B displays the corresponding GSC energy $|\Delta E_{GSC}|$ during small disturbances over time, revealing that the entire energy demand is sustained by the rotor throughout the disturbance period.

When the disturbance causes the frequency deviation of the WSSs to exceed the frequency threshold $|\Delta f_{th}|$, it is classified as a large disturbance. At this point, the DC voltage is stabilized by both the rotor and the BS to achieve cooperative support on the DC side. Since the system's frequency deviation resulting from large disturbances undergoes a process, the proposed control uses a different cooperative strategy before and after reaching the frequency triggering threshold. Figure 6 illustrates the support of power and energy required by the GSC during large disturbances. In Figure 6A, when the system is in state $|\Delta f| < |\Delta f_{th}|$, all the power required by the GSC is supplied by the rotor alone; however, in state $|\Delta f| > |\Delta f_{th}|$, both the rotor and the BS jointly provide

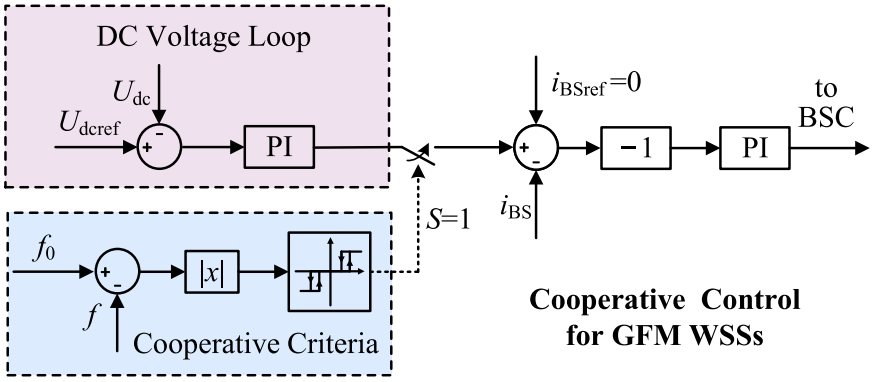

FIGURE 8
Block diagram of the cooperative control for GFM WSS.

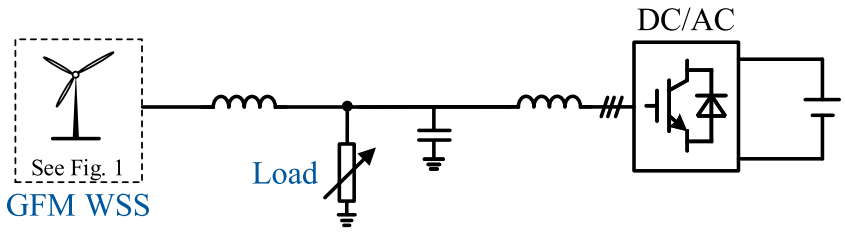

FIGURE 9
Test system of the cooperative control for GFM WSS.

TABLE 1 Main parameters of test system.

Description	Symbol	Value
Initial load power	P_{L0}	400 kW
Initial WSSs power	P_{w0}	200 kW
Initial grid power	P_{g0}	200 kW
Wind speed	v	12 m/s
Initial rotor speed	n_0	89.4 r/min
DC-capacitor	C_{dc}	20 mF
DC-link voltage	U_{dc}	1800 V
Droop coefficient	K_p	0.01 Hz/kW
Rated line voltage	E_N	690 Vrms
Rated frequency	f_N	50 Hz
Frequency deviation threshold upper limit	$\lvert\Delta f_{th}^{h}\rvert$	0.11 Hz
Frequency deviation threshold lower limit	$\lvert\Delta f_{th}^{l}\rvert$	0.09 Hz
Initial battery SOC	SOC	80%

power support for the DC capacitor. The corresponding energy required by the GSC during large disturbances over time is depicted in Figure 6B. In state $|\Delta f| < |\Delta f_{th}|$, all the energy is sourced from the rotor, whereas in state $|\Delta f| > |\Delta f_{th}|$, the BS is activated to supply energy to the DC capacitor in conjunction with the rotor.

The cooperative principle of the proposed cooperative FR control strategy for the wind storage system is shown in Figure 7. When the WSSs encounter disturbances, the rotor first provides FR support power for the DC capacitor, and at the same time, its frequency deviation is measured; if $|\Delta f| < |\Delta f_{th}|$, the BS is disabled and the rotor only supports the disturbed power by sacrificing the rotational speed; if $|\Delta f| > |\Delta f_{th}|$, the BS is enabled, and the rotor and the BS work together to maintain the stability of the DC voltage, which realizes the cooperative support of DC capacitance.

3.2 Cooperative control strategy

Building upon the cooperative principle described above, the control block diagram of the proposed DC side power support cooperative control strategy for GFM WSSs is depicted in Figure 8.

To achieve the control objective of determining whether the BS should be activated based on whether the frequency deviation reaches the frequency threshold $|\Delta f_{th}|$, the BS DC current i_{BS} can be selected as the controlled parameter. In the cooperative control

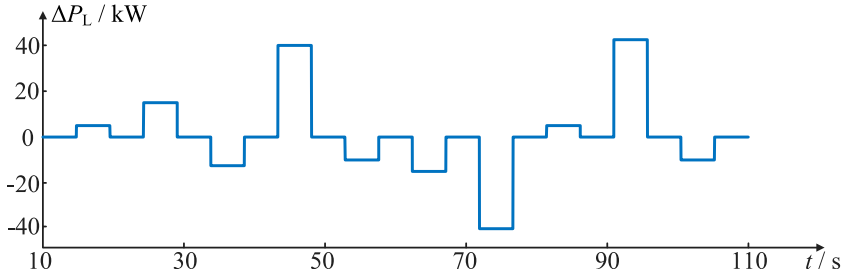

FIGURE 10
Stochastic disturbances.

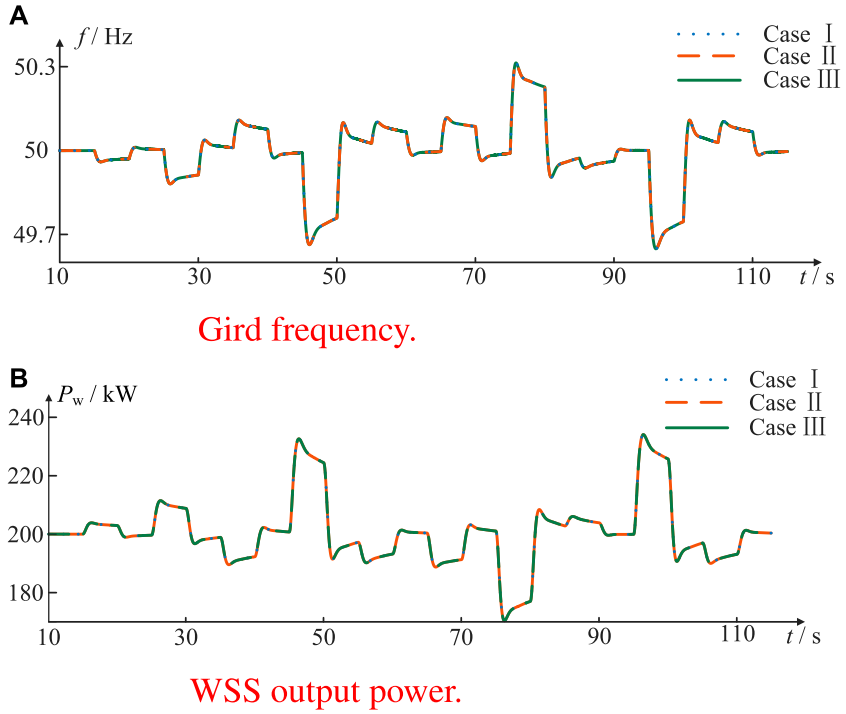

FIGURE 11
Gird-side results under stochastic disturbances. **(A)** Gird frequency. **(B)** WSS output power.

strategy, the reference value of the BS DC current, i_{BSref}, is initially set to 0 since the BS typically remains inactive. Activation of the BS occurs only when a disturbance causes the system deviation to exceed the frequency threshold $|\Delta f_{\mathrm{th}}|$, indicating a large disturbance. To address potential instability issues at the threshold boundary, a hysteresis loop module is implemented to define the cooperative criteria for large disturbances. The design logic of the hysteresis loop module is shown in Eq. 4,

$$S = \begin{cases} 0 & |\Delta f| < \left|\Delta f_{\mathrm{th}}^{\mathrm{l}}\right| \\ 1 & |\Delta f| \geq \left|\Delta f_{\mathrm{th}}^{\mathrm{h}}\right| \end{cases} \tag{4}$$

where S is the flag of the energy storage criterion; $\left|\Delta f_{\mathrm{th}}^{\mathrm{h}}\right|$ is the frequency deviation threshold upper limit and $\left|\Delta f_{\mathrm{th}}^{\mathrm{l}}\right|$ is the frequency deviation threshold lower limit.

When the hysteresis loop module S is at 0, the BS remains inactive; however, when the hysteresis loop module S transitions to 1, the DC voltage loop activates, thereby enabling the BS to provide power support for the DC capacitor.

4 Verification

To validate the effectiveness and superiority of the proposed DC power support cooperative control, this section integrates the GFM WSSs with the grid to evaluate the DC power support characteristics. The constructed test system is illustrated in Figure 9.

In this paper, the test system is constructed within the MATLAB/SIMULINK environment, and the specific parameters are outlined in Table 1. The detailed configuration of the tested

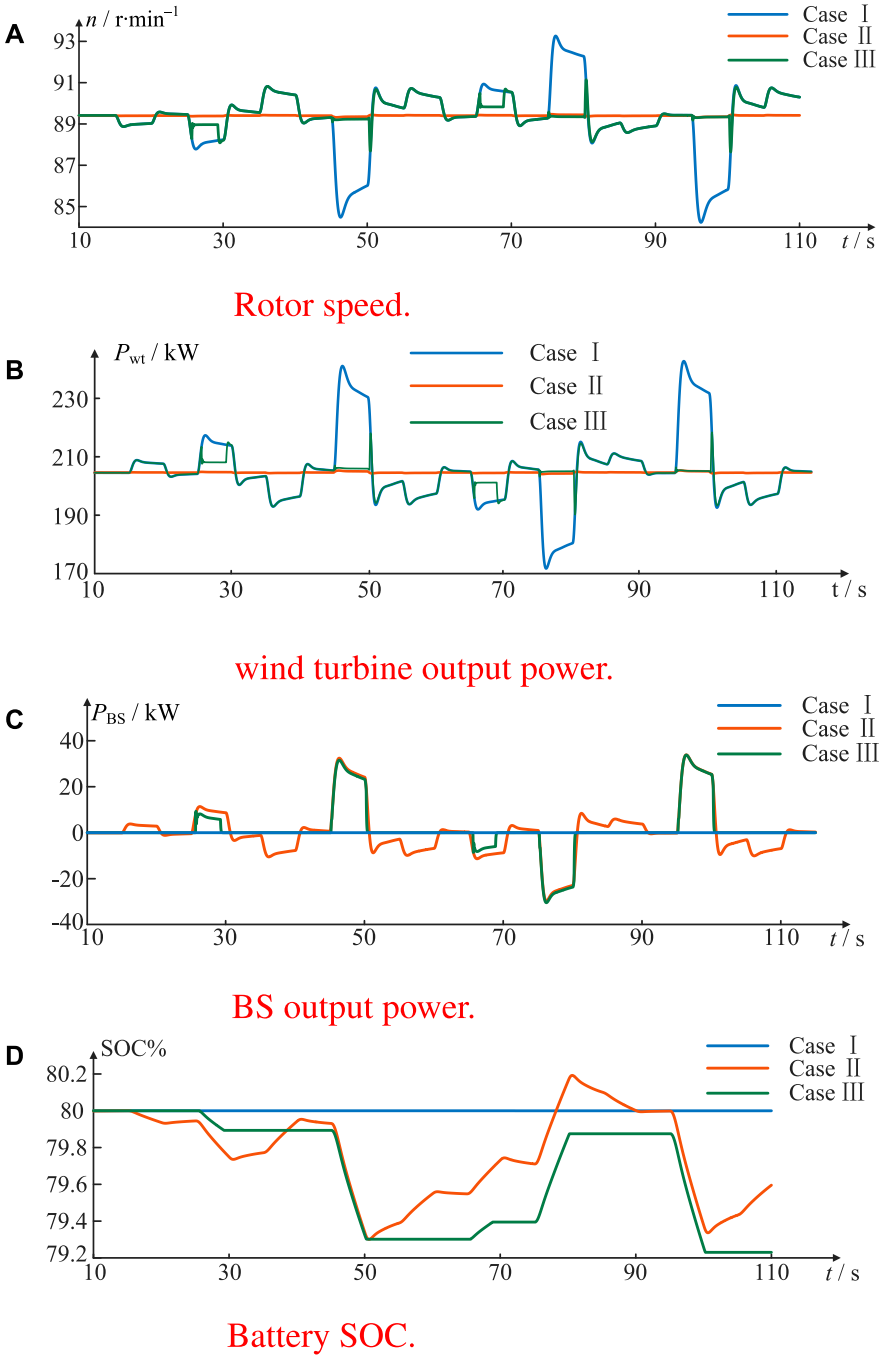

FIGURE 12
DC-side results under stochastic disturbances. **(A)** Rotor speed. **(B)** Wind turbine output power. **(C)** BS output power. **(D)** Battery SOC.

GFM WSSs is depicted in Figure 8. The grid's frequency response characteristics are emulated using an inverter, which is controlled using virtual synchronous generator control.

When a small disturbance occurs, the proposed cooperative control anticipates that the WSSs BS will remain inactive, with the rotor supplying all the necessary support power. Only in the event of a large disturbance causing the frequency deviation to surpass the frequency threshold $|\Delta f_{th}|$, does the BS become operational, collaborating with the rotor to stabilize the DC voltage and achieve cooperative power support on the DC side. To assess the effectiveness of the proposed cooperative control strategy, the control effects of the following three control methods are simulated and analyzed.

- Case I: The BS does not participate in FR and total FR power is provided by the rotor.
- Case II: Immediately upon the occurrence of a grid disturbance, both the rotor and the energy storage system respond promptly.
- Case III: The proposed cooperative control strategy.

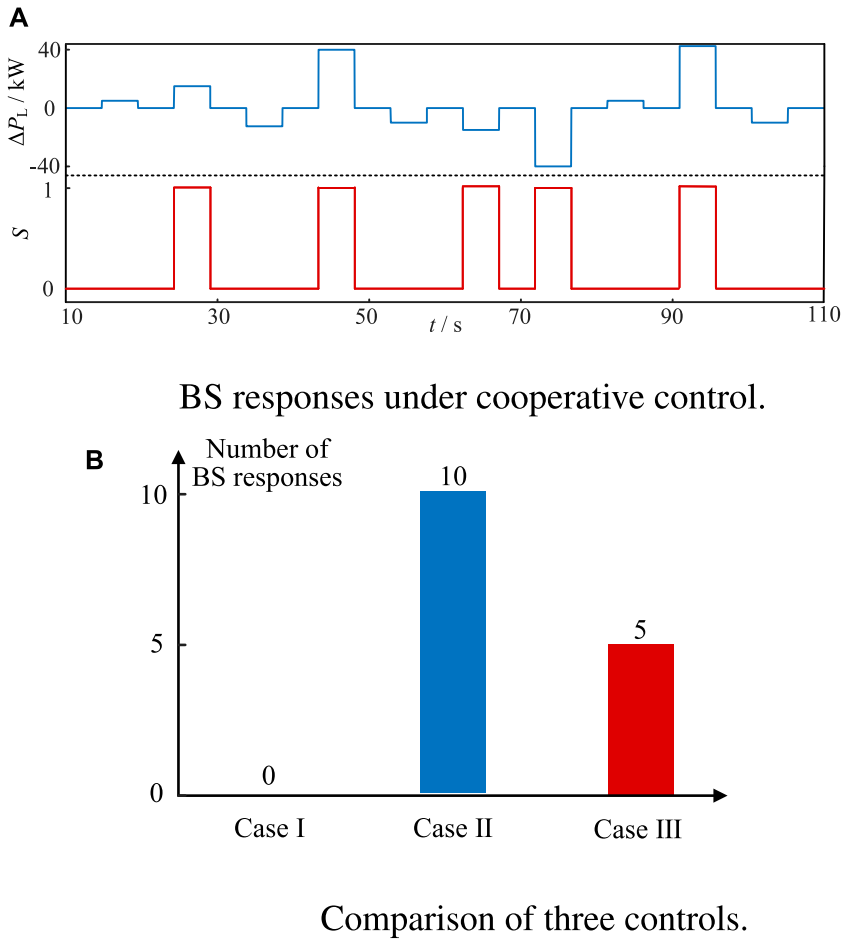

FIGURE 13
Comparison of WSSs BS responses under three controls. **(A)** BS responses under cooperative control. **(B)** Comparison of three controls.

In the initial conditions of the test system, the load power is jointly supported by the WSSs and the grid to ensure the stabilization of the system frequency. Random disturbances, including both large and small disturbances, are set between 10 s and 110 s. The values of these disturbances are in the range of −40 kW–40 kW, as illustrated in Figure 10.

As shown in Figure 11, the grid frequency f and the output power P_w of the WSSs remain consistent across all three control methods. This consistency is attributed to the uniform GSC control strategy employed by all three methods. Moreover, the output power of the WSSs, managed by the GSC to integrate with the grid, is contingent upon the grid-side loads and the GFM control methodology it employs.

In Figures 12A,B, the WSSs rotor speed n and BS power PBS are illustrated. In Case I, grid-side load changes are solely managed by the rotor, resulting in wide fluctuations in rotor speed and potential damage to its mechanical structure. In Case II, the BS responds faster than the rotor to grid-side load changes, leading to frequent charging and discharging cycles of the BS, thus reducing its service life and increasing WSSs' investment costs. However, in Case III, the proposed cooperative control method is employed. Here, the BS responses are minimized while ensuring stable rotor speed. This is achieved by activating the BS only when $|\Delta f| > |\Delta f_{th}|$, and the rotor provides all support power when $|\Delta f| < |\Delta f_{th}|$. Consequently, the proposed method enhances the BS's service life and improves the economic and technological benefits of WSSs, while safeguarding the rotor's mechanical integrity. Figure 12C displays the SOC% of the BS under the three control methods. The proposed cooperative control method notably reduces the time of BS charging and discharging compared to the method where the BS responds to every disturbance.

In Figure 13A, the response of the WSSs BS to load-side disturbances under cooperative control is depicted. It's evident that the BS only reacts to large disturbances under this control scheme. Additionally, Figure 13B compares the response times of the BS under the three control methods. It demonstrates that when confronted with identical disturbance scenarios, cooperative control significantly reduces the number of BS responses, thereby enhancing its service life.

5 Conclusion

This manuscript analyzes the principle of cooperative DC power support for GFM WSSs and proposes a cooperative strategy for GFM

WSSs. The simulation results verify that the proposed control can effectively reduce the number of BS responses. The main conclusions are as follows.

1) The cooperative principle of the GFM WSSs is as follows: for small disturbances, the BS is disabled and total frequency regulation power is provided by the rotor, while for large disturbances, the BS is enabled to cooperatively provide power support with the rotor.
2) Based on the cooperative principle, the proposed cooperative strategy can distinguish between large and small disturbances by using a frequency threshold. Additionally, it incorporates a hysteresis loop module into the cooperative criterion. This module facilitates the cooperative support of both the rotor and the BS on the DC side of the WSSs.
3) The simulation results indicate that the proposed strategy effectively can reduce the times of BS charging and discharging. This improvement contributes to extend the service life of BSs while ensuring that rotor speed remains stable without wide fluctuations.

Data availability statement

The original contributions presented in the study are included in the article/Supplementary Material, further inquiries can be directed to the corresponding author.

Author contributions

XZ: Conceptualization, Data curation, Formal Analysis, Funding acquisition, Investigation, Methodology, Project administration, Resources, Software, Supervision, Validation, Visualization, Writing–original draft, Writing–review and editing. JW: Conceptualization, Methodology, Software, Validation, Writing–original draft, Writing–review and editing, Data curation, Formal Analysis, Investigation. ZG: Data curation, Software, Writing–review and editing, Formal Analysis, Investigation, Methodology. SZ: Formal Analysis, Investigation, Writing–review and editing, Visualization. WT: Supervision, Writing–review and editing, Visualization.

Funding

The author(s) declare that no financial support was received for the research, authorship, and/or publication of this article.

Conflict of interest

The authors declare that the research was conducted in the absence of any commercial or financial relationships that could be construed as a potential conflict of interest.

Publisher's note

References

Ahsan, H., and Mufti, M.-u. D. (2020). Systematic development and application of a fuzzy logic equipped generic energy storage system for dynamic stability reinforcement. *Int. J. Energy Res.* 44, 8974–8987. doi:10.1002/er.5606

Astero, P., and Evens, C. (2020). Optimum operation of battery storage system in frequency containment reserves markets. *IEEE Trans. Smart Grid* 11, 4906–4915. doi:10.1109/tsg.2020.2997924

Bao, W., Ding, L., Kang, Y. C., and Sun, L. (2022). Closed-loop synthetic inertia control for wind turbine generators in association with slightly over-speeded deloading operation. *IEEE Trans. Power Syst.* 38, 5022–5032. doi:10.1109/tpwrs.2022.3224431

Dhiman, H. S., and Deb, D. (2020). Wake management based life enhancement of battery energy storage system for hybrid wind farms. *Renew. Sustain. Energy Rev.* 130, 109912. doi:10.1016/j.rser.2020.109912

Huang, L., Wu, C., Zhou, D., Chen, L., Pagnani, D., and Blaabjerg, F. (2023). Challenges and potential solutions of grid-forming converters applied to wind power generation system—an overview. *Front. Energy Res.* 11, 1040781. doi:10.3389/fenrg.2023.1040781

Jiao, Y., and Nian, H. (2020). Grid-forming control for dfig based wind farms to enhance the stability of lcc-hvdc. *IEEE Access* 8, 156752–156762. doi:10.1109/access.2020.3019691

Lin, Z., and Liu, X. (2020). Wind power forecasting of an offshore wind turbine based on high-frequency scada data and deep learning neural network. *Energy* 201, 117693. doi:10.1016/j.energy.2020.117693

Liu, H., Li, M., Liu, L., and Shi, J. (2021). Frequency trajectory planning-based transient frequency regulation strategy for wind turbine systems. *IEEE J. Emerg. Sel. Top. Power Electron.* 10, 3987–4000. doi:10.1109/jestpe.2021.3113822

Liu, Y., Wu, X., Du, J., Song, Z., and Wu, G. (2020). Optimal sizing of a wind-energy storage system considering battery life. *Renew. Energy* 147, 2470–2483. doi:10.1016/j.renene.2019.09.123

Meng, J., Wang, D., Wang, Y., Guo, F., and Yu, J. (2023). An improved damping adaptive grid-forming control for black start of permanent magnet synchronous generator wind turbines supported with battery energy storage system. *IET Generation, Transm. Distribution* 17, 354–366. doi:10.1049/gtd2.12753

Mohamed, M. M., El Zoghby, H. M., Sharaf, S. M., and Mosa, M. A. (2022). Optimal virtual synchronous generator control of battery/supercapacitor hybrid energy storage system for frequency response enhancement of photovoltaic/diesel microgrid. *J. Energy Storage* 51, 104317. doi:10.1016/j.est.2022.104317

Sang, S., Pei, B., Huang, J., Zhang, L., and Xue, X. (2021). Low-voltage ride-through of the novel voltage source-controlled pmsg-based wind turbine based on switching the virtual resistor. *Appl. Sci.* 11, 6204. doi:10.3390/app11136204

Shadoul, M., Ahshan, R., AlAbri, R. S., Al-Badi, A., Albadi, M., and Jamil, M. (2022). A comprehensive review on a virtual-synchronous generator: topologies, control orders and techniques, energy storages, and applications. *Energies* 15, 8406. doi:10.3390/en15228406

Sun, M., Sun, Y., Chen, L., Zou, Z., Min, Y., Liu, R., et al. (2022). Novel temporary frequency support control strategy of wind turbine generator considering coordination with synchronous generator. *IEEE Trans. Sustain. Energy* 13, 1011–1020. doi:10.1109/tste.2022.3142914

Xiong, L., Liu, X., Zhang, D., and Liu, Y. (2020). Rapid power compensation-based frequency response strategy for low-inertia power systems. *IEEE J. Emerg. Sel. Top. Power Electron.* 9, 4500–4513. doi:10.1109/jestpe.2020.3032063

Xiong, L., Liu, X., Zhao, C., and Zhuo, F. (2019). A fast and robust real-time detection algorithm of decaying dc transient and harmonic components in three-phase systems. *IEEE Trans. Power Electron.* 35, 3332–3336. doi:10.1109/tpel.2019.2940891

Xiong, L., Zhuo, F., Wang, F., Liu, X., Chen, Y., Zhu, M., et al. (2015). Static synchronous generator model: a new perspective to investigate dynamic characteristics and stability issues of grid-tied pwm inverter. *IEEE Trans. Power Electron.* 31, 6264–6280. doi:10.1109/tpel.2015.2498933

Yang, J., Yang, T., Luo, L., and Peng, L. (2023). Tracking-dispatch of a combined wind-storage system based on model predictive control and two-layer fuzzy control strategy. *Prot. Control Mod. Power Syst.* 8, 58–16. doi:10.1186/s41601-023-00334-6

Yao, L., Wang, W., Liu, J., Wang, Y., and Chen, Z. (2024). Economic optimal control of source-storage collaboration based on wind power forecasting for transient frequency regulation. *J. Energy Storage* 84, 111002. doi:10.1016/j.est.2024.111002

Zeng, W., Li, R., Huang, L., Liu, C., and Cai, X. (2021). Approach to inertial compensation of hvdc offshore wind farms by mmc with ultracapacitor energy storage integration. *IEEE Trans. Industrial Electron.* 69, 12988–12998. doi:10.1109/tie.2021.3134092

Zhao, F., Wang, X., Zhou, Z., Harnefors, L., Svensson, J. R., Kocewiak, Ł. H., et al. (2021). Control interaction modeling and analysis of grid-forming battery energy storage system for offshore wind power plant. *IEEE Trans. Power Syst.* 37, 497–507. doi:10.1109/tpwrs.2021.3096850